Optimization of Inkjet Printing of Patch Antennas on Low-Cost Fibrous Substrates

Hossein Saghlatoon, Lauri Sydänheimo, *Member, IEEE*, Leena Ukkonen, *Member, IEEE*, and Manos Tentzeris, *Fellow, IEEE*

***Abstract*—In this letter, the inkjet-printing procedure is used to implement microwave circuits on low-cost fibrous substrate, cardboard. As a first step for environmentally friendly electronics applications, the high-frequency properties of the cardboard substrate are extracted using the two-transmission-line method and dielectric probe measurement. To provide an accurate model for the inkjet-printed conductors, the conductivity and thickness of the printed silver traces are analyzed. The surface of the substrate is pretreated using a dielectric ink to reduce the penetration of the conductor ink into the fibrous substrate and to diminish the conductor loss at high frequencies. As a technology demonstrator, a patch antenna is printed on a cardboard substrate, and the simulation and measurement results are compared to study the reliability of the obtained parameters. After initial experimental verification, simulation models were fine-tuned in order to provide a predictive method for design and fabrication of low-cost RF circuits. The achieved model can be used to design and fabricate low-cost RF structures on fibrous environmentally friendly substrates.**

***Index Terms*—Dielectric characterization, green electronics, inkjet printing, low-cost substrate, paper RF, patch antenna, silver ink, surface treatment, two transmission lines method.**

I. Introduction

AS AN organic substrate, paper has a great potential for the realization of environmentally friendly and recyclable electronics [1], [2]. It is tempting to use paper as a substrate for electronic circuits because it is ultra-low-cost, recyclable, available everywhere, and compatible with printing [3]. Additive printing technologies, such as inkjet printing, feature the capability to increase the fabrication speed and enhance the production versatility, both features that are critical for mass production. Moreover, inkjet printing has been an enabling technology to print electronics on unconventional substrates such as wood, ceramic, and paper [3]–[5]. The electrical properties of the low-cost fibrous types of paper, such as cardboard, should be characterized, especially in microwave frequencies because the RF properties of different paper materials are not identical [3]. In addition, it is challenging to effectively fabricate circuits on fibrous substrates using inkjet printing because the printed ink penetrates into the substrate and reduces the conductivity and quality of the printed pattern [6].

In this letter, one typical cardboard paper material is used as the substrate and silver nanoparticle ink as the conductor. The rest of this letter is organized as follows. In Section II, the specifics of the cardboard electrical characterization technique are discussed. Then, the measurement results for the conductivity, thickness, and surface roughness of inkjet-printed silver traces before and after treatment of the substrate are proposed according to Section III. Section IV discusses the design of a patch antenna according the obtained parameters, and the effect of inaccuracies in the fabrication and measurement procedures. Finally, conclusions are presented in Section V.

II. RF Characterization of the Cardboard

To enable the effective implementation of efficient microwave structures on a cardboard substrate, its RF properties have to be measured and analyzed. There are different ways to characterize an unknown substrate such as split-cylinder resonator, ring resonator, and other high-Q structures [7], [8]. One of the most accurate methods is the two-transmission-line method. In this method, two identical microstrip lines with different lengths are implemented on the substrate. The effective permittivity $(\varepsilon_{\rm eff})$ of the substrate can be obtained from the phase difference of the signals, and the loss tangent is acquired from the insertion loss. It is not necessary to de-embed the effect of SMA connectors and junctions because all the calculations are based on the transmission-line length difference effectively removing these parasitic effects [8], [9]. Using (1) and (2) the effective permittivity and total loss can be calculated, respectively

$$\varepsilon_{\rm eff} = \left(\frac{\Delta\theta \times C}{2\pi f \times \Delta l}\right)^2 \tag{1}$$

$$\alpha = \frac{\ln \frac{\left|S_{21}^{\rm long}\right|}{\left|S_{21}^{\rm short}\right|}}{\Delta l} \tag{2}$$

where C is the free-space speed of light, $\Delta\theta$ is the phase difference of the output signals for the long and the short lengths, f is the frequency, and Δl is the length difference of the two microstrip lines [8], [10].

By knowing the total loss (α) and conductor loss, the dielectric loss and then the loss tangent can be determined. The total loss is the summation of dielectric loss, conductor loss, and radiation loss. The radiation loss is very low and can be neglected from the calculations because the lengths of the lines are relatively small. In this case, to have a high efficient traveling wave

Manuscript received December 13, 2013; revised February 20, 2014 and April 04, 2014; accepted April 17, 2014. Date of publication May 08, 2014; date of current version May 22, 2014.

H. Saghlatoon, L. Sydänheimo, and L. Ukkonen are with the Tampere University of Technology, 33720 Tampere, Finland (e-mail: hossein.saghlatoon@tut.fi; lauri.sydanheimo@tut.fi; leena.ukkonen@tut.fi).

M. M. Tentzeris is with the Georgia Institute of Technology, Atlanta, GA 30332-250 USA (e-mail: etentze@ece.gatech.edu).

Color versions of one or more of the figures in this letter are available online at http://ieeexplore.ieee.org.

Digital Object Identifier 10.1109/LAWP.2014.2322572

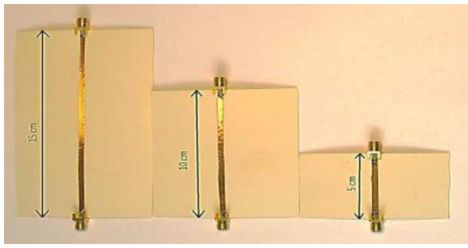

Fig. 1. Implemented microstrip lines on cardboard.

antenna, the length of the lines should be $5\ \lambda$ to $10\ \lambda$. The conductor loss is dependent on the physical properties of the conductor, such as the conductivity and the width of the line. If the properties of the conductor are known, the conductor loss is apparent. The conductor loss of a certain transmission line can be obtained using

$$R_s = \sqrt{\frac{\omega\mu_0}{2\sigma}} \tag{3}$$

$$\alpha_c = \frac{R_s}{Z_0 W} \tag{4}$$

where ω is the angular frequency, σ is the conductivity of the conductor, Z_0 is the characteristic impedance of the line, and W is the width of the microstrip line. Moreover, the loss tangent can be obtained using (5) which is valid for microstrip lines [10]

$$\tan\delta = \frac{\alpha_{\rm d} \times 2\sqrt{\varepsilon_{\rm eff}}(\varepsilon_r - 1)}{K_0\varepsilon_{\rm r}(\varepsilon_{\rm eff} - 1)} \tag{5}$$

where $\alpha_{\rm d}$ is the dielectric loss, $\varepsilon_{\rm r}$ is the relative permittivity of the substrate, $\varepsilon_{\rm eff}$ is the effective relative permittivity of the substrate, and K_0 is the phase constant in free space [10].

For the characterization of the highly fibrous cardboard (Stora Enso packaging thin paper), three microstrip lines with 15-, 10-, and 5-cm lengths were realized on its surface utilizing a 50-μ m-thick copper tape with bulk conductivity of 5.8×10^7 S/m, terminated in 50-Ω SMA conductors, and having the same width of 2 mm for a characteristic impedance of 50 Ω, as shown in Fig. 1. The longest line is almost $0.15\ \lambda$; hence, the assumption for low radiation loss is acceptable. For higher measurement reliability, S-parameters for the three different lengths were compared one by one utilizing an Agilent PNA E8358A two-port vector network analyzer (VNA) between 500 MHz and 3 GHz. To realize the accuracy of this method, the relative permittivity and loss tangent were measured using Agilent 85070 Dielectric Probe Kit in the same frequency interval. The results for the average permittivity and loss tangent of the substrate using these two methods are depicted in Fig. 2. The results are in a sufficiently good agreement. Depending on the density and water content of cardboard, its permittivity can vary between 1.2 and 1.5 [11].

III. Characterizing the Printed Silver Ink

The next important step for the inkjet printing of RF structures on cardboard is the characterization of the conductivity and the realized thickness of the printed conductive traces. NPS-JL silver ink with 55.5wt% metal content was used to print using Dimatix DMP-2831 inkjet material printer. The volume and diameter of each droplet was 10 pL and 140 μm,

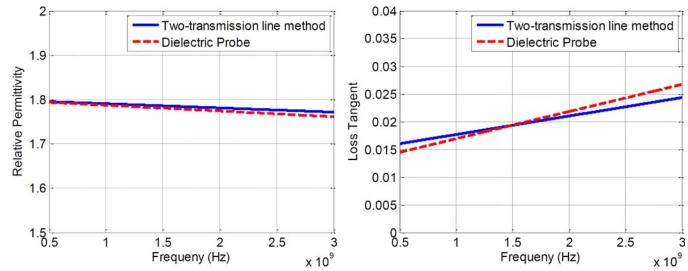

(a) (b)

Fig. 2. Measured properties of cardboard. (a) Relative permittivity. (b) Loss tangent.

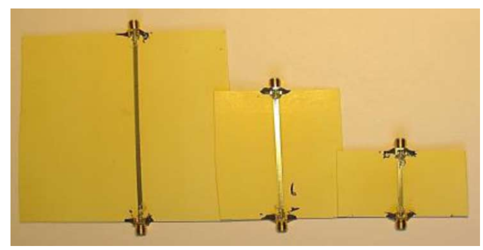

Fig. 3. Fabricated inkjet microstrip lines on cardboard.

respectively. To optimize the conductivity value, a sintering process at 150 °C for 1 h with air circulation was applied, and each RF pattern was printed [12]. For appropriate conductivity, each pattern was printed in four cycles. In each cycle, two layers of silver ink were printed and sintered, so at the end there were eight layers of silver ink with the total thickness of 3 μm on cardboard.

Following this process, three microstrip lines with different lengths were printed on cardboard as shown in Fig. 3. The dimensions of these lines are identical to the copper tape versions for the purpose of easier comparison. In this case, the dielectric loss is known, and by measuring the total loss, the conductor loss can be obtained. The acquired value for the conductivity of these structures is 1×10^7 S/m.

Considering the cardboard substrate, there are numerous reasons that led to a reduced value of conductivity compared to the maximum achievable value (3.3×10^7 S/m) presented by the manufacturer. These include the lower realized conductor thickness compared to the skin depth and the high surface roughness. The thickness of the printed silver ink on cardboard was measured using an optical microscope. The ink penetrates into the cardboard due to its highly fibrous nature [6]. By penetration of the ink into the fibrous substrate, the conductivity diminishes because the printed silver nanoparticles cannot make a uniform conductor. In addition, cardboard is not a good thermal conductor; hence, in the sintering process, the printed silver ink is not cured properly. Therefore, there is a demand to make the surface smooth and ink proof. It can be easily seen in Fig. 4 that without a surface treatment approach, the ink penetration into the substrate is around 55 μm. Usually, different dielectric inks are utilized to treat the surface [13], [14]. We used a conventional primer (composed of tetrahydrofurfuryl acrylate, ethoxylated trimethylolpropane triacrylate, 2-hydroxy-2-methyl-1-phenyl-propan-1-one, and bis-phenylphosphineoxide

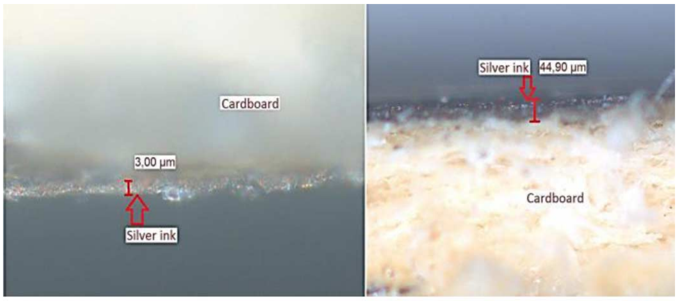

(a) (b)

Fig. 4. Measured thickness of the ink (a) after treatment and (b) before treatment.

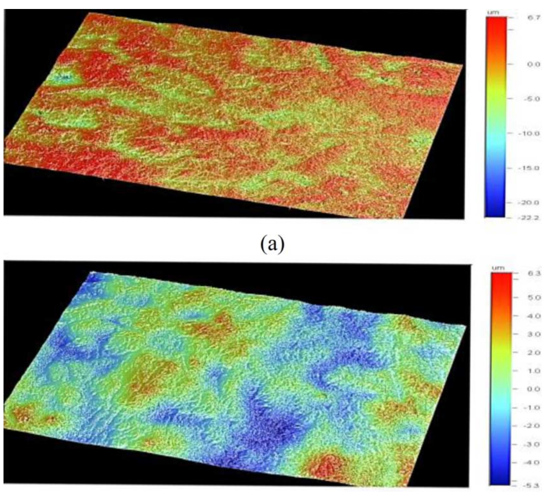

(a)

(b)

Fig. 5. Scanned surface of cardboard using optical profilometer. (a) Before treatment. (b) After treatment.

[6]) to prepare a smooth surface for silver ink [6]. For this purpose, four layers of primer with 1016 dpi resolution were printed separately on the rough surface of cardboard. After the printed deposition of each layer, it was cured using ultraviolet light (UV) for 15 min, and then 1 h at 150 °C in an oven. Afterwards, silver ink was inkjet-printed on the treated surface utilizing the conventional sintering approach.

The surface roughness of the printed silver ink on the treated and untreated cardboard was scanned using an optical profilometer with results shown in Fig. 5. As can be deduced, the peak-to-valley distance is around 39 μm before treatment, which is improved to 11.5 μm after treatment. Moreover, the mean roughness and root mean squared roughness are improved from 1.68 and 2.13 μm before treatment to 1.3 and 1.62 μm after treatment, respectively. After the preparation of the smooth and ink-proof surface, the same microstrip lines were printed to analyze the new value of conductivity, which was found to be almost double $(2 \times 10^7$ S/m$)$. The other important parameter for the printed silver ink traces for high-frequency designs is the conductor thickness uniformity. The cross section of the treated cardboard with printed silver ink is shown in Fig. 4. As can be seen, the thickness is almost uniform in the whole printed area and equal to 3 μm.

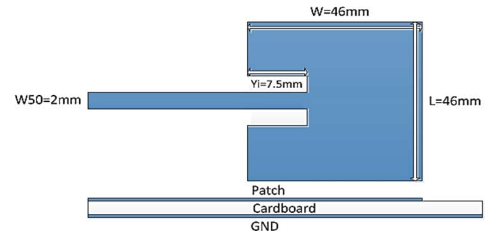

Fig. 6. Configuration of the inkjet-printed patch antenna on cardboard.

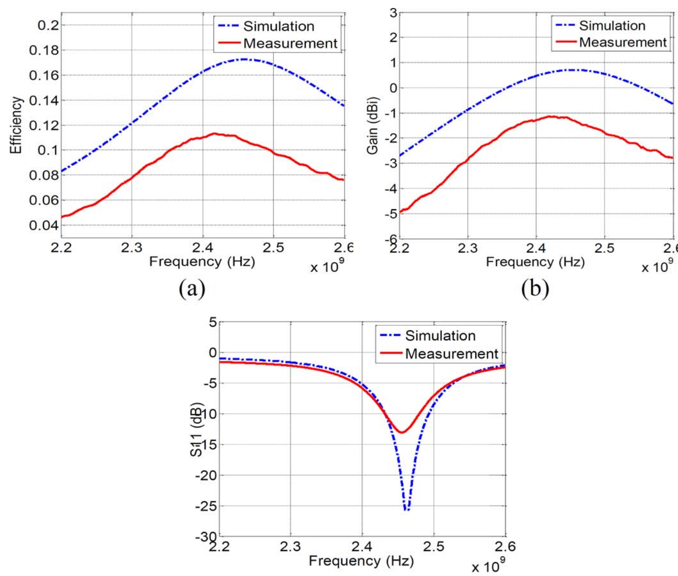

(a) (b)

(c)

Fig. 7. Simulation and measurement results for the proposed antenna. (a) Radiation efficiency. (b) Radiation gain. (c) Return loss.

TABLE I
OBTAINED VALUES FOR DIFFERENT PARAMETERS OF CARDBOARD AND SILVER INK

Measured parameter	value at 2.45 GHz
Relative permittivity of cardboard	1.78
Loss tangent of cardboard	0.025
Thickness of cardboard	560 um
Conductivity of silver ink	2×10^7 S/m
Thickness of silver ink	3 um

IV. IMPLEMENTATION OF THE 2.45 GHz PATCH ANTENNA

As a proof of concept and without loss of generality, a microstrip patch antenna for 2.45 GHz with inset feeding was designed for the acquired properties of the cardboard and of the silver ink traces presented in Table I. The antenna is designed to operate in the TM_{010} excitation mode, and its dimensions are shown in Fig. 6.

This configuration was simulated using the 3-D full-wave electromagnetic simulator Ansys HFSS based on finite element method, while the inkjet-printed prototype was measured using the near-field measurement equipment Satimo Starlab. The simulation and measurement results for the radiation gain, radiation efficiency, and return loss are shown in Fig. 7. As can be seen, there are slight discrepancies between the simulation and measurement results. We believe these discrepancies arise due to layer-to-layer alignment error and printer tolerances $(\pm 25\ \mu\mathrm{m})$. However, it can be observed that this phenomenon increases the

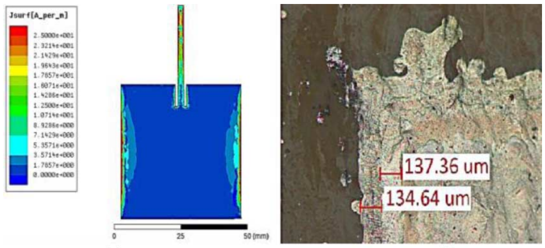

Fig. 8. (a) Current distribution in the patch antenna at 2.45 GHz. (b) Misalignment of the printed layers.

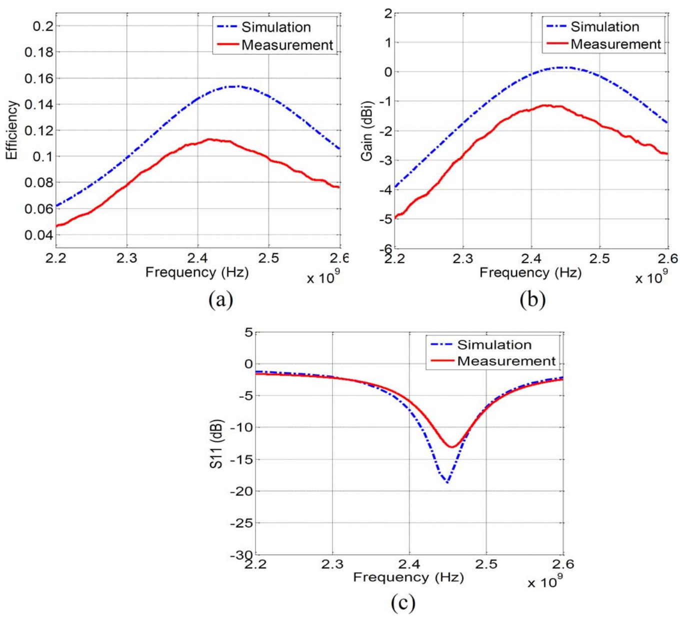

Fig. 9. Simulation and measurement results with the optimized model. (a) Radiation efficiency. (b) Radiation gain. (c) Return loss.

losses in the radiating edges of the patch antenna and of the feeding line.

The results for the measured misalignment of different layers using an optical microscope and for the simulated of the current distribution magnitude are shown in Fig. 8. As can be seen in Fig. 8(b), the misalignments of different layers are approximately in the range of 130 μm and shown with the red shift. To compensate for the effect of misaligned layers in the simulation model, the conductivity of the radiating edges and of the feeding line edges is reduced. The width and conductivity of the added part in the simulations is 130 μm and 0.5×10^7 S/m. The aforementioned two-transmission-line method was used to measure the conductivity of the misaligned part.

Fig. 9 depicts the simulation results for the radiation efficiency, radiation gain, and return loss for the new corrected model. With this model, the matching between the simulated and measured efficiency is improved by 1.5%, and the gain by 1 dB. Another potential source of measurement error is the inaccuracy of the near-field measurement device, which is ± 0.7 dB for the peak gain at 1880 MHz. Compared to the simulation model, the roughness of the printed structure is another source of error that will be modeled in the further studies.

V. Conclusion

We have presented a novel method for the optimization of inkjet printing of RF structures on fibrous substrates. As a proof of concept, the properties of a typically highly fibrous cardboard substrate as well as of the inkjet-printed silver traces are accurately characterized up to 3 GHz. A smoothness/substrate hermeticity enhancing approach for the cardboard is presented, and numerous uncertainties of inkjet printing approach are modeled. The acquired values for the permittivity and loss tangent of the cardboard, as well as the thickness and the conductivity values for the printed silver traces are 1.78, 0.025, 3 μm, and 2×10^7 S/m, respectively. Based on the developed method, a patch antenna is simulated, fabricated with inkjet printing on cardboard, and then measured. Finally, the simulation and measurement results were compared, and acceptable agreement is achieved. It can be concluded that the optimized model for cardboard and silver ink can be used in the fabrication and optimization of RF structures on ultra-low-cost highly fibrous substrates, such as cardboard.

References

[1] S. Palacios *et al.*, “Inkjet-printed planar antenna for a wireless sensor on paper operating at wi-fi frequency,” in *Proc. IEEE APSURSI*, Jul. 2012, pp. 1–2.

[2] M. Irimia-Vladu, “Green electronics: biodegradable and biocompatible materials and devices for sustainable future,” *Chem. Soc. Rev.*, vol. 43, no. 2, pp. 588–610, 2014.

[3] L. Yang, A. Rida, R. Vyas, and M. M. Tentzeris, “RFID Tag and RF structures on paper substrates using inkjet-printing technology,” *IEEE Trans. Microw. Theory Tech.*, vol. 55, no. 12, pp. 2894–2901, Dec. 2007.

[4] J. Virkki, J. Virtanen, L. Sydanheimo, L. Ukkonen, and M. M. Tentzeris, “Embedding inkjet-printed antennas into plywood structures for identification and sensing,” in *Proc. IEEE RFID-TA*, Nov. 2012, pp. 34–39.

[5] A. A. Babar *et al.*, “Inkjet-printable UHF RFID tag antenna on a flexible ceramic-polymer composite substrate,” in *IEEE MTT-S Microw. Symp. Dig.*, Jun. 2012, pp. 1–3.

[6] A. Denneulin, J. Bras, A. Blayo, and C. N. Neuman, “Substrate pretreatment of flexible material for printed electronics with carbon nanotube based ink,” *Appl. Surface Sci.*, vol. 257, no. 8, pp. 3645–3651, 2011.

[7] L. Yang and M. M. Tentzeris, “Design and characterization of novel paper-based inkjet-printed RFID and microwave structures for telecommunication and sensing applications,” in *Proc. IEEE MTT-S Int. Microw. Symp.*, Jun. 2007, pp. 1633–1636.

[8] S. H. Chang, H. Kuan, H. W. Wu, R. Y. Yang, and M. H. Weng, “Determination of microwave dielectric constant by two microstrip line method combined with EM simulation,” *Microw. Opt. Technol. Lett.*, vol. 48, no. 11, pp. 2199–2201, 2006.

[9] N. K. Das, S. M. Voda, and D. M. Pozar, “Two methods for the measurement of substrate dielectric constant,” *IEEE Trans. Microw. Theory Tech.*, vol. MTT-35, no. 7, pp. 636–642, Jul. 1987.

[10] D. M. Pozar, *Microwave Engineering*, 1st ed. New York, NY, USA: Wiley, 1990, ch. 4, pp. 126–204.

[11] M. Sivakumar and D. D. Deavours, “A dual-resonant microstrip antenna for paperboard in the cold chain,” in *Proc. IEEE Sarnoff Symp.*, 2008, pp. 1–5.

[12] Harima, “NPS-JL silver nanoparticle ink,” NanoPaste Series, Metal Paste for Thin Film Formation, Datasheet, 2012.

[13] R. Bollström *et al.*, “A multilayer coated fiber-based substrate suitable for printed functionality,” *Organic Electron.*, vol. 10, no. 5, pp. 1020–1023, 2009.

[14] S. M. Hurst, B. Farshchian, J. Choi, J. Kim, and S. Park, “A universally applicable method for fabricating superhydrophobic polymer surfaces,” *Colloids Surfaces A, Physicochem. Eng. Aspects*, vol. 407, pp. 85–90, 2012.